

Robust and sparse Gaussian graphical modeling under cell-wise contamination

Shota Katayama¹, Hironori Fujisawa^{2,3} and Mathias Drton⁴

¹Department of Industrial Engineering and Economics, Tokyo Institute of Technology, Japan

²The Institute of Statistical Mathematics, Japan

³Nagoya University Graduate School of Medicine, Japan

⁴Department of Statistics, University of Washington, USA

Abstract

Graphical modeling explores dependences among a collection of variables by inferring a graph that encodes pairwise conditional independences. For jointly Gaussian variables, this translates into detecting the support of the precision matrix. Many modern applications feature high-dimensional and contaminated data that complicate this task. In particular, traditional robust methods that down-weight entire observation vectors are often inappropriate as high-dimensional data may feature partial contamination in many observations. We tackle this problem by giving a robust method for sparse precision matrix estimation based on the γ -divergence under a cell-wise contamination model. Simulation studies demonstrate that our procedure outperforms existing methods especially for highly contaminated data.

keywords: cell-wise contamination; Gaussian graphical modeling; precision matrix; sparsity; robust inference

1 Introduction

Let $\mathbf{Y} = (Y_1, \dots, Y_p)^T$ be a p -dimensional random vector representing a multivariate observation. The conditional independence graph of \mathbf{Y} is the undirected graph $G = (V, E)$ whose vertex set $V = \{1, \dots, p\}$ indexes the individual variables and whose edge set E indicates conditional dependences among them. More precisely, $(i, j) \notin E$ if and only if Y_i and Y_j are conditionally independent given $Y_{V \setminus \{i, j\}} = \{Y_k : k \neq i, j\}$. For a Gaussian vector, the edge set E corresponds to the support of the precision matrix. Indeed, it is well known that if \mathbf{Y} follows a multivariate Gaussian distribution $N_p(\boldsymbol{\mu}, \boldsymbol{\Sigma})$ with mean vector $\boldsymbol{\mu}$ and covariance matrix $\boldsymbol{\Sigma}$, then $(i, j) \notin E$ if and only if $\boldsymbol{\Omega}_{ij} = 0$, where $\boldsymbol{\Omega} = \boldsymbol{\Sigma}^{-1}$.

Inference of the conditional independence graph sheds light on direct as opposed to indirect interactions and has received much recent attention (Drton & Maathuis, 2017). In particular, for high-dimensional Gaussian problems, several techniques have been developed that exploit available sparsity in inference of the support of the precision matrix Ω . Meinshausen & Bühlmann (2006) suggested fitting node-wise linear regression models with ℓ_1 penalty to recover the support of each row. Yuan & Lin (2007), Banerjee et al. (2008) and Friedman et al. (2008) considered the graphical lasso (Glasso) that involves the ℓ_1 penalized log-likelihood function. Cai et al. (2011) proposed the constrained ℓ_1 minimization for inverse matrix estimation (CLIME), which may be formulated as a linear program. Yet other approaches can be found in Yuan (2009), Peng et al. (2009), Zhang & Zou (2014), Kahre et al. (2015), Liu & Luo (2015), and Lin et al. (2016).

In fields such as bioinformatics and economics, data are often not only high-dimensional but also subject to contamination. While suitable for high dimensionality, the above mentioned techniques are sensitive to contamination. Moreover, traditional robust methods may not be appropriate when the number of variables is large. Indeed, they are based on the model in which an observation vector is either without contamination or fully contaminated. Hence, an observation vector is treated as an outlier even if only one of many variables is contaminated. As a result these methods down-weight the entire vector regardless of whether it contains ‘clean’ values for some variables. Such information loss can become fatal as the dimension increases. As a more realistic model in high dimensional data, Alqallaf et al. (2002) considered cell-wise contamination: The observations $\mathbf{X}_1, \dots, \mathbf{X}_n$ with p variables are generated by

$$\mathbf{X}_i = (\mathbf{I}_p - \mathbf{E}_i)\mathbf{Y}_i + \mathbf{E}_i\mathbf{Z}_i, \quad i = 1, \dots, n. \quad (1)$$

Here, \mathbf{I}_p is the $p \times p$ identity matrix and each $\mathbf{E}_i = \text{diag}(E_{i1}, \dots, E_{ip})$ is a diagonal random matrix with the E_{ij} ’s independent and Bernoulli distributed with $P(E_{ij} = 1) = \varepsilon_j$. The random vectors \mathbf{Y}_i and \mathbf{Z}_i are independent, and $\mathbf{Y}_i \sim N_p(\boldsymbol{\mu}, \boldsymbol{\Sigma})$ corresponds to a clean sample while \mathbf{Z}_i makes contaminations in some elements of \mathbf{X}_i .

Our goal is to develop a robust estimation method for the conditional independence graph G of \mathbf{Y}_i from the cell-wise contaminated observations \mathbf{X}_i . Techniques such as node-wise regression, Glasso and CLIME process an estimate of the covariance matrix. Our strategy is thus simply to apply these procedures using a covariance matrix estimator that is robust against cell-wise contamination. However, while many researchers have considered the traditional ‘whole-vector’ contamination framework (see, e.g., Maronna et al., 2006, Chapter 6), there are fewer existing methods for cell-wise contamination. Specifically, we are aware of

three approaches, namely, use of alternative t -distributions (Finegold & Drton, 2011, 2014), use of rank correlations (Loh & Tan, 2015; Öllerer & Croux, 2015), and a pairwise covariance estimation method by Tarr et al. (2016) who adopt an idea of Gnanadesikan & Kettenring (1972). In contrast, in this paper, we provide a robust covariance matrix estimator via γ -divergence as proposed by Fujisawa & Eguchi (2008). The γ -divergence can automatically reduce the impact of contaminations, and it is known to be robust even when the number of contaminations is large.

The rest of this paper is structured as follows. We review some graph estimation methods in Section 2.1 and the γ -divergence in Section 2.2. In Section 3, the robust covariance matrix estimator via γ -divergence is proposed and some of the existing competitors are introduced. Numerical experiments that illustrate the benefits of our new method are presented in Section 4. Concluding remarks are given in Section 5.

2 Preliminaries

2.1 Graph estimation

For concise presentation, we focus on node-wise regression, Glasso and CLIME. Let $\hat{\Sigma}$ be an estimator of Σ . For index sets A and B , define $\hat{\Sigma}_{A,B}$ as the sub-matrix of $\hat{\Sigma}$ with the rows in A and the columns in B . We use the shorthand $\setminus j$ for the set $V \setminus \{j\}$, so that $\hat{\Sigma}_{\setminus j, \setminus j}$ denotes the sub-matrix with both rows and columns in $V \setminus \{j\}$. In ℓ_1 penalized node-wise regression, one finds

$$\hat{\beta}^{(j)} = \operatorname{argmin}_{\beta \in \mathbb{R}^{p-1}} \frac{1}{2} \beta^T \hat{\Sigma}_{\setminus j, \setminus j} \beta - \hat{\Sigma}_{j, \setminus j} \beta + \lambda \|\beta\|_1, \quad j = 1, \dots, p,$$

where the tuning parameter $\lambda > 0$ controls the strength of the penalty $\|\beta\|_1$. Large λ yields high sparsity of $\hat{\beta}^{(j)}$. After obtaining $\hat{\beta}^{(1)}, \dots, \hat{\beta}^{(p)}$, the edge set E is estimated by the ‘‘AND’’ rule $\hat{E} = \{(i, j) : \hat{\beta}_i^{(j)} \neq 0 \text{ and } \hat{\beta}_j^{(i)} \neq 0\}$ or the ‘‘OR’’ rule $\hat{E} = \{(i, j) : \hat{\beta}_i^{(j)} \neq 0 \text{ or } \hat{\beta}_j^{(i)} \neq 0\}$. Node-wise regression is well-defined for any positive semidefinite estimate $\hat{\Sigma}$.

The Glasso estimator is obtained by solving

$$\hat{\Omega}^{\text{Glasso}} = \operatorname{argmin}_{\Omega \in \mathbb{R}^{p \times p}} \operatorname{tr} \hat{\Sigma} \Omega - \log |\Omega| + \lambda \|\Omega\|_1, \quad (2)$$

where $\|\Omega\|_1$ is the element-wise ℓ_1 norm of Ω and $\lambda > 0$ is a tuning parameter that controls the sparsity of Ω . The edge set may be estimated by $\hat{E} = \{(i, j) : \hat{\Omega}_{ij} \neq 0\}$. Efficient algorithms for the Glasso are given in Friedman et al. (2008) and Hsieh et al. (2011). For

convergence, the former requires $\hat{\Sigma} + \lambda \mathbf{I}_p$ to be positive semidefinite while the latter requires the same for $\hat{\Sigma}$.

Finally, we review the CLIME method. Let

$$\hat{\Omega}^0 = \underset{\Omega \in \mathbb{R}^{p \times p}}{\operatorname{argmin}} \|\Omega\|_1 \quad \text{subject to} \quad \|\hat{\Sigma}\Omega - \mathbf{I}_p\|_\infty \leq \lambda, \quad (3)$$

where $\|\cdot\|_\infty$ means the element-wise infinity norm. Generally, $\hat{\Omega}^0 = (\hat{\omega}_{ij}^0)$ is not symmetric. The CLIME is defined through a simple symmetrization, namely,

$$\hat{\Omega}_{ij}^{\text{CLIME}} = \hat{\omega}_{ij}^0 I(|\hat{\omega}_{ij}^0| \leq |\hat{\omega}_{ji}^0|) + \hat{\omega}_{ji}^0 I(|\hat{\omega}_{ij}^0| > |\hat{\omega}_{ji}^0|), \quad i, j = 1, \dots, p,$$

and the edge set is estimated as in Glasso. Cai et al. (2011) translated the matrix optimization problem from (3) into p vector optimization problems. Each of them can be solved by linear programming. The CLIME essentially needs the positive definiteness of $\hat{\Sigma}$. Without it, the optimization problem may be infeasible or return inadequate solutions.

2.2 Robust inference via γ -divergence

Let f and f_n be the data generating and empirical densities, respectively. In robust inference one typically assumes that $f = (1 - \varepsilon)g + \varepsilon h$, where g is the density of clean data, h is the density of contamination, and $\varepsilon \geq 0$ is the contamination level. For estimation of g , consider a model with densities g_θ indexed by the parameter θ . The Kullback-Leibler (KL) divergence between f_n and g_θ results in a biased estimate unless $\varepsilon = 0$. To overcome it, Fujisawa & Eguchi (2008) proposed the γ -divergence given by

$$d_\gamma(f_n, g_\theta) = -\frac{1}{\gamma} \log \int f_n(x) g_\theta(x)^\gamma dx + \frac{1}{1 + \gamma} \log \int g_\theta(x)^{1+\gamma} dx,$$

where $\gamma > 0$ is a constant that controls the trade-off between efficiency and robustness. In fact, the γ -divergence is equivalent to the KL divergence when $\gamma \rightarrow 0$. The estimator given by minimizing $d_\gamma(f_n, g_\theta)$ over a possible parameter space is highly robust. Roughly speaking, in the limiting case $n \rightarrow \infty$, $d_\gamma(f_n, g_\theta)$ can be regarded as $d_\gamma(f, g_\theta)$, and

$$d_\gamma(f, g_\theta) = -\frac{1}{\gamma} \log \left\{ (1 - \varepsilon) \int g(x) g_\theta(x)^\gamma dx + \varepsilon \nu(\theta; \gamma) \right\} + \frac{1}{1 + \gamma} \log \int g_\theta(x)^{1+\gamma} dx,$$

where $\nu(\theta; \gamma) = \int h(x) g_\theta(x)^\gamma dx$. The γ -divergence successfully provides robust estimates whenever $\nu(\theta; \gamma) \approx 0$ over the parameter space considered. In such a case, we see that $d_\gamma(f, g_\theta) \approx d_\gamma(g, g_\theta) - (1/\gamma) \log(1 - \varepsilon)$, where the contamination density h is automati-

cally ignored, so that the minimizer of $d_\gamma(f, g_\theta)$ is approximately equal to the minimizer of $d_\gamma(g, g_\theta)$. This is a favorable property, because when $g = g_{\theta^*}$, the minimizer of $d_\gamma(g, g_\theta)$ is θ^* . Fortunately, $\nu(\theta; \gamma)$ is close to zero when h lies in the tail of g_θ^γ . To illustrate this fact, assume for a moment that g_θ is the density of $N(\theta, 1)$. If h is the density of $N(\alpha, 1)$, then $\nu(\theta; \gamma) = c_{1,\gamma} \exp\{-c_{2,\gamma}(\alpha - \theta)^2\}$ for some $c_{1,\gamma}, c_{2,\gamma} > 0$. Thus, $\nu(\theta; \gamma)$ is small whenever α is not too close to the set of parameters θ that determine the better fitting densities g_θ .

3 Methods

3.1 Proposed methodology

As noted in Section 2.1, we seek a robust covariance estimate $\hat{\Sigma}$ for use in graph estimation. In this section, we construct such an estimate via the γ -divergence. Our estimator $\hat{\Sigma}$ is constructed in an element-wise fashion and exhibits robustness to cell-wise contamination. We begin by writing each covariance as

$$\Sigma_{jk} = \sqrt{\sigma_{jj}}\sqrt{\sigma_{kk}}\rho_{jk}, \quad (4)$$

where $\sigma_{jj} = \text{Var}(Y_{ij})$, $\sigma_{kk} = \text{Var}(Y_{ik})$ and $\rho_{jk} = \text{Corr}(Y_{ij}, Y_{ik})$, for $j, k = 1, \dots, p$. Here, $\mathbf{Y}_i = (Y_{i1}, \dots, Y_{ip})^T$ is the i -th unobserved clean sample in (1). We now derive estimates of the variances and the correlation in (4) based on the observations $\mathbf{X}_i = (X_{i1}, \dots, X_{ip})^T$, which under cell-wise contamination may have some of their elements corrupted.

Fixing a coordinate $j \in \{1, \dots, p\}$, let $g_{(\mu_j, \sigma_{jj})}$ be the density of $N(\mu_j, \sigma_{jj})$, and let $f_n^{(j)}$ be the empirical density of X_{1j}, \dots, X_{nj} . The robust estimators of μ_j and σ_{jj} based on γ -divergence are given by

$$\begin{aligned} (\hat{\mu}_j, \hat{\sigma}_{jj}) &= \underset{\mu_j, \sigma_{jj}}{\text{argmin}} d_\gamma(f_n^{(j)}, g_{(\mu_j, \sigma_{jj})}), \\ d_\gamma(f_n^{(j)}, g_{(\mu_j, \sigma_{jj})}) &= -\frac{1}{\gamma} \log \sum_{i=1}^n \exp \left\{ -\frac{\gamma}{2\sigma_{jj}} (X_{ij} - \mu_j)^2 \right\} + \frac{1}{2(1+\gamma)} \log \sigma_{jj}. \end{aligned}$$

Fujisawa & Eguchi (2008) gave an efficient iterative algorithm to compute $(\hat{\mu}_j, \hat{\sigma}_{jj})$. Let μ_j^t and σ_{jj}^t denote the t -th values starting from initializations μ_j^0 and σ_{jj}^0 . The algorithm repeats the following steps until convergence:

$$\mu_j^{t+1} \leftarrow \sum_{i=1}^n w_{ij}^t X_{ij}, \quad \sigma_{jj}^{t+1} \leftarrow (1+\gamma) \sum_{i=1}^n w_{ij}^t (X_{ij} - \mu_j^{t+1})^2,$$

where the weights are updated as

$$w_{ij}^t = \exp \left\{ -\frac{\gamma}{2\sigma_{jj}^t} (X_{ij} - \mu_j^t)^2 \right\} / \sum_{i=1}^n \exp \left\{ -\frac{\gamma}{2\sigma_{jj}^t} (X_{ij} - \mu_j^t)^2 \right\}.$$

We take the median of X_{1j}, \dots, X_{nj} as μ_j^0 and the median absolute deviation (MAD) as σ_{jj}^0 .

After $\hat{\mu}_j$ and $\hat{\sigma}_{jj}$ are obtained for $j = 1, \dots, p$, we estimate each correlation ρ_{jk} from the standardized observations $Z_{ij} = (X_{ij} - \hat{\mu}_j) / \sqrt{\hat{\sigma}_{jj}}$. Let $h_{\rho_{jk}}$ be the bivariate standardized normal density with correlation ρ_{jk} , and let $f_n^{(j,k)}$ be the empirical density of $(Z_{1j}, Z_{1k}), \dots, (Z_{nj}, Z_{nk})$. Our correlation estimator is

$$\hat{\rho}_{jk} = \operatorname{argmin}_{|\rho_{jk}| < 1} d_\gamma(f_n^{(j,k)}, h_{\rho_{jk}}), \quad (5)$$

$$d_\gamma(f_n^{(j,k)}, h_{\rho_{jk}}) = -\frac{1}{\gamma} \log \sum_{i=1}^n \exp \left\{ -\frac{\gamma}{2(1 - \rho_{jk}^2)} (Z_{ij}^2 + Z_{ik}^2 - 2\rho_{jk} Z_{ij} Z_{ik}) \right\} + \frac{1}{2(1 + \gamma)} \log |1 - \rho_{jk}^2|.$$

The required univariate optimization problem can be solved with standard techniques. We provide a projected gradient descent algorithm in [Appendix A](#). Finally, we obtain the estimator of Σ_{jk} as $\hat{\Sigma}_{jk} = \sqrt{\hat{\sigma}_{jj}} \sqrt{\hat{\sigma}_{kk}} \hat{\rho}_{jk}$.

3.2 Existing works

Some other estimators of Σ have been proposed under the cell-wise contamination. [Öllerer & Croux \(2015\)](#) and [Loh & Tan \(2015\)](#) considered use of rank correlations. Based on the decomposition (4), [Loh & Tan \(2015\)](#) estimated the scale by MAD, and used the Kendall's tau and Spearman's rho to estimate the correlation. [Öllerer & Croux \(2015\)](#) proposed to use Q_n from [Rousseeuw & Croux \(1993\)](#) for the scale, and estimate the correlation by the Gaussian rank correlation from [Boudt et al. \(2012\)](#). [Tarr et al. \(2016\)](#) directly estimate Σ_{jk} following the pairwise approach of [Gnanadesikan & Kettenring \(1972\)](#), which is based on the identity

$$\Sigma_{jk} = \operatorname{Cov}(Y_j, Y_k) = \frac{1}{4\alpha_j \alpha_k} \left\{ \operatorname{Var}(\alpha_j Y_j + \alpha_k Y_k) - \operatorname{Var}(\alpha_j Y_j - \alpha_k Y_k) \right\}, \quad (6)$$

where $\alpha_j = 1/\sqrt{\operatorname{Var}(Y_j)}$. [Tarr et al. \(2016\)](#) proposed to estimate the population variance from the contaminated data using robust scales such as Q_n , the τ -scale of [Maronna & Zamar \(2002\)](#), and P_n from [Tarr et al. \(2012\)](#).

3.3 Projection of covariance matrix estimate

We cannot directly plug an estimate of Σ into the methods introduced in Section 2.1 if it is not positive semidefinite. The node-wise regression and Glasso require a positive semidefinite estimate, and CLIME needs a positive definite one. The estimate proposed by Öllerer & Croux (2015) is always positive semidefinite, but this may not be true for the other estimates including the one we proposed. However, if an estimate $\hat{\Sigma}$ is not positive semidefinite, we may project it onto the set of positive (semi)definite matrices. Different approaches to this projection have been considered (Zhao et al., 2014). We will simply proceed by solving the problem

$$\min_{\mathbf{S}} \|\mathbf{S} - \hat{\Sigma}\|_F \quad \text{subject to } \mathbf{S} \geq \delta \mathbf{I}_p,$$

where $\delta \geq 0$, $\|\cdot\|_F$ denotes the Frobenius norm and $\mathbf{S} \geq \delta \mathbf{I}_p$ means that $\mathbf{S} - \delta \mathbf{I}_p$ is positive semidefinite. The solution can be calculated by applying the singular value decomposition to $\hat{\Sigma}$ and then replacing the singular values λ_j by $\max(\lambda_j, \delta)$ for each $j = 1, \dots, p$. We set $\delta = 0$ throughout the paper.

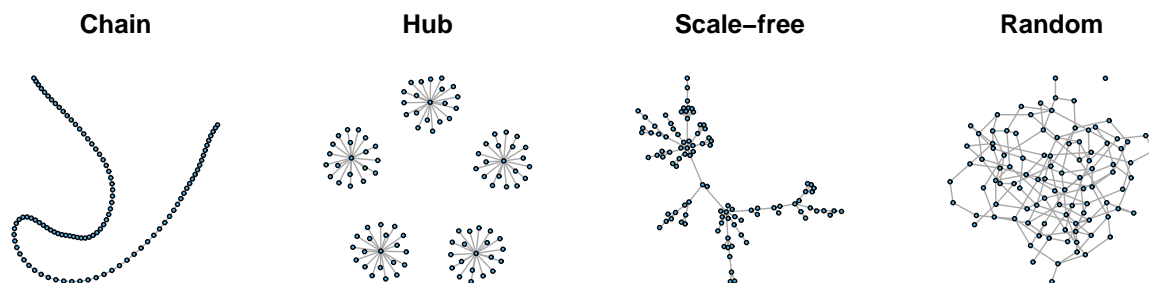


Figure 1: Four types of true graphs.

4 Empirical results

4.1 Simulations

We provide some simulation results to illustrate the effectiveness of our method for the graph estimation problem.¹ We generated 200 observations from the cell-wise contamination model

¹R code to implement our method is available at https://github.com/shkatayama/robust_graphical_model.

(1) with $p = 100$, $\boldsymbol{\mu} = \mathbf{0}$ and the equal contamination level $\varepsilon := \varepsilon_1 = \dots = \varepsilon_p$. Both asymmetric and symmetric contaminations are considered, that is, $100\varepsilon\%$ of observations in each variable are corrupted by samples from $N(10, 1)$ in the asymmetric scenario, while half of the corruption are from $N(-10, 1)$ in the other case. The true covariance matrix $\boldsymbol{\Sigma}$ determines the true graph structure via $\boldsymbol{\Omega} = \boldsymbol{\Sigma}^{-1}$. We considered four types of true graphs as shown in Figure 1. The chain, hub and scale-free graphs were generated by `huge` package (Zhao et al., 2012), and the random graph was made as in Liu et al. (2012).

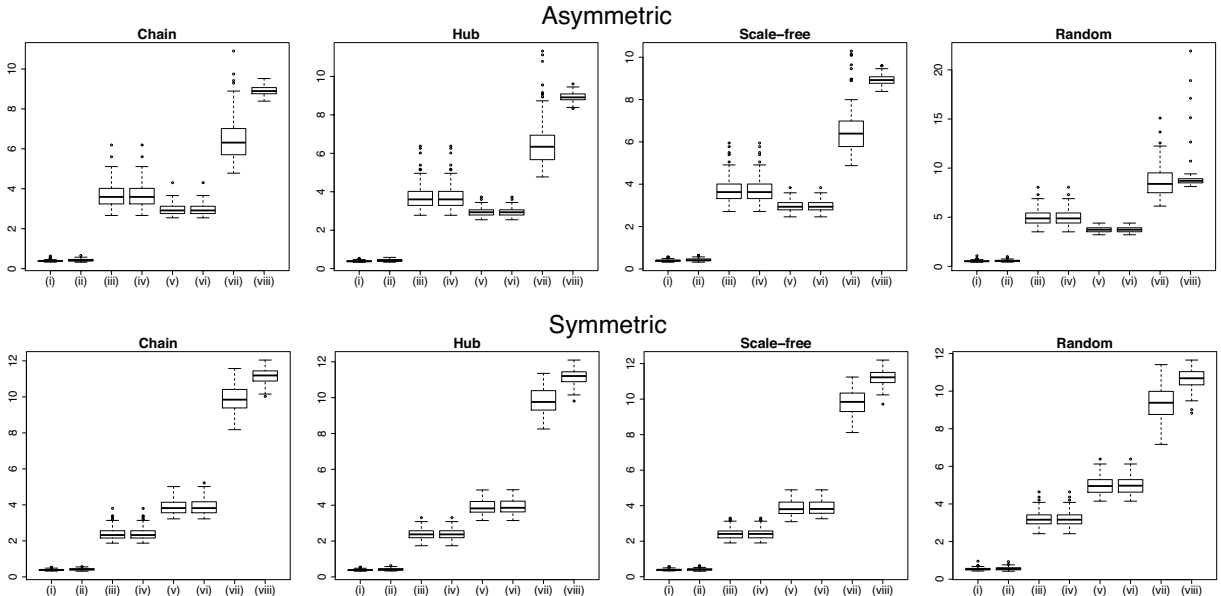


Figure 2: Boxplots for our estimators with (i) $\gamma = 0.3$ and (ii) $\gamma = 0.5$, (iii) Kendall’s tau, (iv) Spearman’s rho, (v) Gaussian rank, and pairwise approach with (vi) Q_n , (vii) τ -scale and (viii) P_n (adaptively trimmed version) when $\varepsilon = 0.25$.

First, we compare our estimator to the existing ones that we described in Section 3.2. Performance is evaluated using the measure $\|\hat{\boldsymbol{\Sigma}} - \boldsymbol{\Sigma}\|_\infty$ that the accuracy of the resulting graph depends on (Cai et al., 2011; Jeng & Daye, 2011; Ravikumar et al., 2011). Figure 2 shows boxplots based on 100 simulations with $\varepsilon = 0.25$. Our estimator can be seen to greatly outperform the others in all cases. Kendall’s tau and Spearman’s rho prefer the symmetric contaminations, while the opposite holds for the Gaussian rank. The pairwise approach performs poorly unless Q_n is used.

Next, we consider graph estimation. We focus on the better performing competitors, namely, Kendall’s tau, Gaussian rank and Q_n . Spearman’s rho is omitted as it behaved similarly to Kendall’s tau. Furthermore, we restrict attention to `Glasso`—the other methods are discussed in the supplement, with similar conclusions. The `Glasso` was implemented using

the QUIC package of [Hsieh et al. \(2011\)](#). Figure 3 illustrates edge recovery via an averaged ROC curve from 100 simulations. Each individual ROC curve is a plot of $(\text{FPR}(\lambda), \text{TPR}(\lambda))$ versus the tuning parameter λ in (2). Here, for the estimated edge set $\hat{E} = \hat{E}(\lambda)$ and the true edge set $E = \{(i, j) : \Omega_{ij} \neq 0\}$, $\text{FPR}(\lambda) = |\hat{E} \cap E^c|/|E^c|$ and $\text{TPR}(\lambda) = |\hat{E} \cap E|/|E|$. Inspecting Figure 3, we can see that our method strongly outperforms the competitors for all graphs considered, particularly when observations are highly and symmetrically corrupted. It is also shown that the recovery performance of our method hardly changes as the contamination level increases ($\varepsilon = 0.05, 0.15, 0.25$).

In order to realize the strengths of our method in practice, a specific value of the tuning parameter λ in Glasso needs to be selected. We studied this for a 2-fold cross validation approach in which the observations are randomly split into two folds with nearly equal size. A robust covariance matrix $\hat{\Sigma}_k$ is calculated on each fold $k = 1, 2$. Let

$$L(\lambda) = \text{tr} \left(\hat{\Sigma}_2 \hat{\Omega}_1(\lambda) \right) - \log \det \hat{\Omega}_1(\lambda)$$

be the negative log-likelihood with $\hat{\Omega}_1(\lambda)$ estimated only from $\hat{\Sigma}_1$. We then select the tuning parameter by minimizing $L(\lambda)$ over a grid of choices for λ . The main reason for the small number of folds is that the γ -divergence needs a sufficient sample size in each fold for the convergence $d_\gamma(f_n, g_\theta) \rightarrow d_\gamma(f, g_\theta)$ to hold; recall Section 2.2. [Bickel & Levina \(2008\)](#) justify the procedure in high-dimensional covariance estimation.

Table 1 summarizes the performance of Glasso with tuning parameter selection when $\varepsilon = 0.25$. Similar experiments for $\varepsilon = 0.05$ and $\varepsilon = 0.15$ are described in the supplement. The grid for λ is chosen as 10 equally spaced values on the log scale between $\lambda_{\max} = \|\hat{\Sigma} - \text{diag}(\hat{\Sigma})\|_\infty$ and $0.05\lambda_{\max}$. Table 1 reports the mean squared error (MSE) given by $\|\hat{\Omega} - \Omega\|_F/p$ in addition to TPR and FPR. Our method and Q_n show high TPR and low FPR, which suggests that the tuning parameter is appropriately selected. Compared with Q_n , our method has lower FPR while keeping TPR high. Moreover, our method entirely outperforms the competitors in MSE.

4.2 Real data analysis

We consider two applications to gene expression data with smaller dimension and stock data with large dimension. Both data sets have heavy tailed distributions in some variables. The first example, an Arabidopsis thaliana data set, is from [Wille et al. \(2004\)](#) with $n = 118$ observations for $p = 39$ genes. The 39 genes are divided into the three groups: 19 relating to the methylerythritol phosphate (MEP) pathway in the chloroplast, 15 relating to the

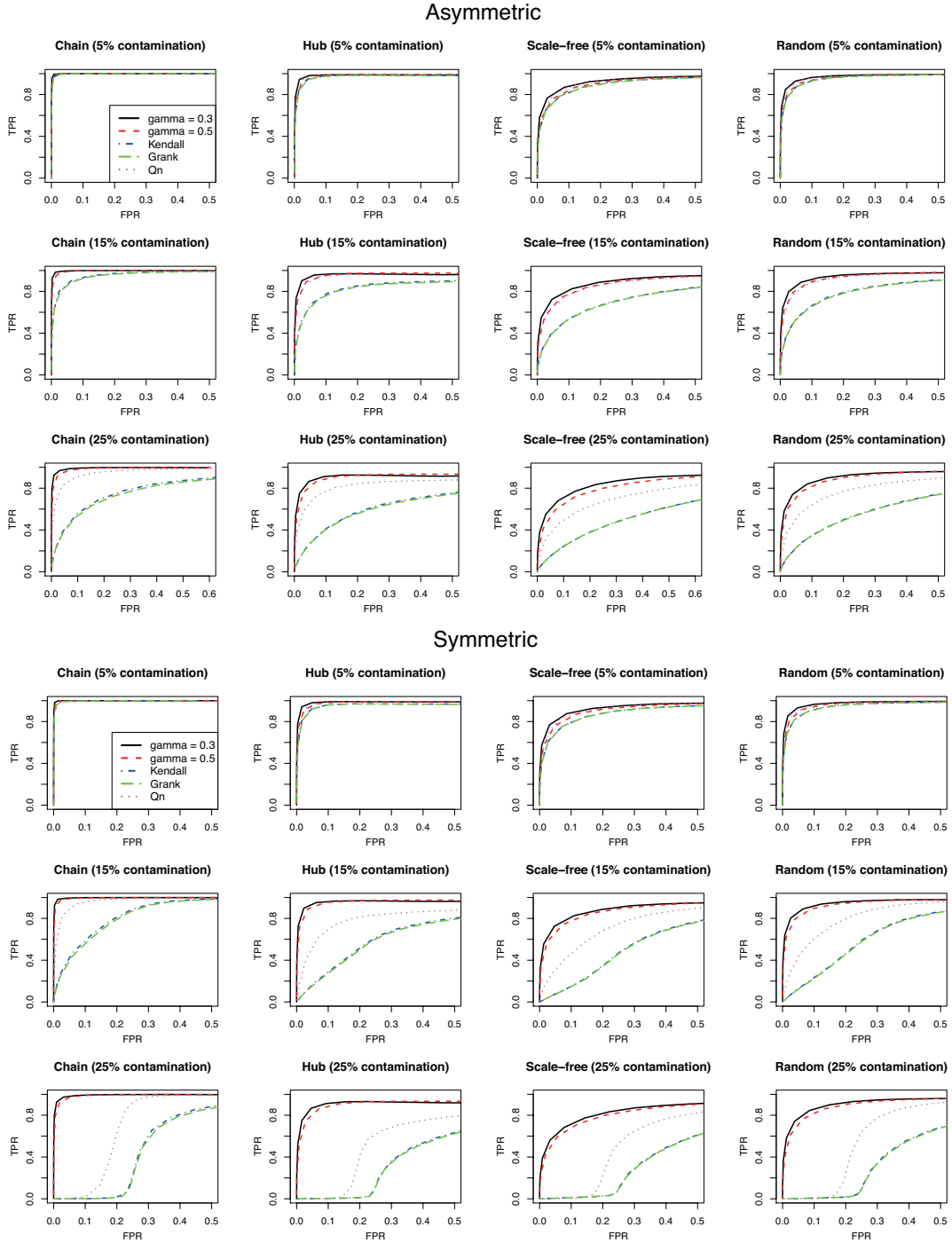


Figure 3: ROC curves for Glasso based on our estimators with $\gamma = 0.3$ and $\gamma = 0.5$, Kendall's tau, Gaussian rank and pairwise approach with Q_n , for asymmetric and symmetric contaminations at the different levels ($\varepsilon = 0.05, 0.15, 0.25$).

Table 1: Quantitative performance of Glasso based on the 5 methods when $\varepsilon = 0.25$ and the tuning parameter is selected by 2-fold cross validation. Each value shows the mean (standard deviation) on 100 simulated data sets.

	Chain			Hub			Scale-free			Random				
	MSE	TPR	FPR	MSE	TPR	FPR	MSE	TPR	FPR	MSE	TPR	FPR		
Asym.	$\gamma = 0.3$	0.074	0.992	0.106	0.084	0.903	0.092	0.053	0.584	0.044	0.049	0.753	0.063	
		(0.004)	(0.011)	(0.025)	(0.002)	(0.045)	(0.024)	(0.002)	(0.103)	(0.020)	(0.005)	(0.165)	(0.031)	
	$\gamma = 0.5$	0.085	0.972	0.064	0.089	0.843	0.063	0.055	0.458	0.029	0.051	0.692	0.045	
		(0.003)	(0.026)	(0.023)	(0.002)	(0.083)	(0.026)	(0.002)	(0.114)	(0.017)	(0.002)	(0.079)	(0.021)	
	Kendall	0.141	0.161	0.009	0.130	0.085	0.010	0.096	0.033	0.007	0.086	0.058	0.008	
		(0.001)	(0.098)	(0.008)	(0.001)	(0.073)	(0.009)	(0.001)	(0.032)	(0.007)	(0.001)	(0.045)	(0.008)	
	Grank	0.142	0.145	0.008	0.130	0.069	0.007	0.096	0.035	0.006	0.086	0.056	0.007	
		(0.001)	(0.097)	(0.008)	(0.001)	(0.056)	(0.006)	(0.001)	(0.036)	(0.006)	(0.001)	(0.047)	(0.008)	
	Q_n	0.140	0.941	0.132	0.129	0.800	0.133	0.098	0.488	0.084	0.086	0.665	0.112	
		(0.001)	(0.028)	(0.035)	(0.001)	(0.067)	(0.042)	(0.001)	(0.090)	(0.028)	(0.001)	(0.080)	(0.037)	
	Sym.	$\gamma = 0.3$	0.046	0.821	0.079	0.084	0.907	0.094	0.053	0.595	0.047	0.046	0.825	0.078
			(0.002)	(0.038)	(0.020)	(0.002)	(0.037)	(0.023)	(0.002)	(0.068)	(0.018)	(0.002)	(0.045)	(0.020)
$\gamma = 0.5$		0.050	0.700	0.049	0.088	0.852	0.069	0.055	0.436	0.025	0.050	0.707	0.049	
		(0.002)	(0.082)	(0.021)	(0.002)	(0.075)	(0.028)	(0.002)	(0.102)	(0.014)	(0.002)	(0.083)	(0.022)	
Kendall		0.077	0.061	0.243	0.119	0.070	0.242	0.084	0.052	0.241	0.077	0.058	0.243	
		(0.001)	(0.029)	(0.008)	(0.001)	(0.042)	(0.009)	(0.001)	(0.027)	(0.008)	(0.001)	(0.031)	(0.009)	
Grank		0.077	0.057	0.243	0.120	0.059	0.241	0.084	0.051	0.241	0.077	0.054	0.242	
		(0.001)	(0.027)	(0.008)	(0.001)	(0.040)	(0.009)	(0.001)	(0.026)	(0.009)	(0.001)	(0.029)	(0.010)	
Q_n		0.082	0.744	0.292	0.127	0.653	0.267	0.094	0.505	0.248	0.082	0.742	0.288	
		(0.002)	(0.073)	(0.028)	(0.001)	(0.065)	(0.024)	(0.001)	(0.096)	(0.025)	(0.002)	(0.065)	(0.027)	

mevalonate acid (MVA) pathway in the cytoplasm and 5 in the mitochondria. A dense network within each pathway is expected, but several connections between them have also been reported and discussed in [Wille et al. \(2004\)](#).

The estimated graphs are shown in Figure 4. Before robust covariance estimation, we standardized the data using median and MAD. The tuning parameter of Glasso was selected to obtain 30 edges which is roughly number of edges considered in [Wille et al. \(2004\)](#). We can see from Figure 4 that our method and Q_n identify a connection between the MEP and MVA pathways but Kendall’s tau and Gaussian rank do not. There are slight differences between our method and Q_n . Our method outputs more dense networks within both MEP and MVA pathways, while Q_n connects AACT1 and HDS. The two methods agree that AACT1 is the hub connecting the two pathways. Though [Wille et al. \(2004\)](#) have reported that HMGR1 is also a hub, if we trust our robust analysis, HMGR1 may link to the MEP pathway just through AACT1.

The second example is data on the daily closing prices of the S&P 500 stocks from January 1, 2003 to January 1, 2008. Preprocessing as in [Zhao et al. \(2012\)](#), there are $n = 1257$ observations for $p = 452$ stocks. The stocks are divided into 10 Global Industry Classification Standard (GICS) sectors. We proceeded as in the previous application but selected the tuning parameter to have a total of 2,500 edges, which results in well-clustered structure. Figure 5 illustrates the results, now also considering $\gamma = 0.1$. Stocks in the same

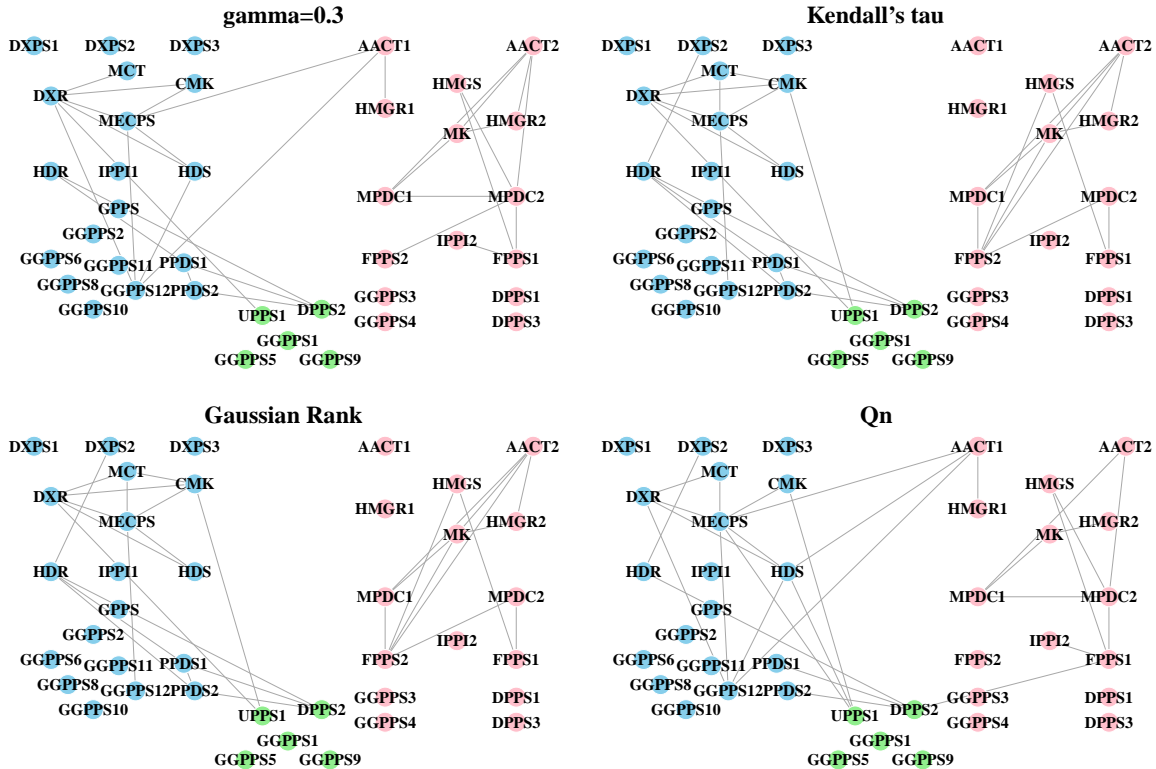


Figure 4: Graphs estimated with Glasso based on our estimator ($\gamma = 0.3$), Kendall’s tau, Gaussian Rank and pairwise approach with Q_n for the Arabidopsis thaliana data set. Each node corresponds to a gene, and each graph has 30 edges. Genes colored blue and red are in the MEP and MVA pathways, respectively. Mitochondria genes are colored green.

GICS sector are shown in the same color. Although the estimated graphs are quite similar, only our method with $\gamma = 0.1$ identifies a direct connection between a stock in the “Utilities” (blue) sector and a stock in the “Materials” (red) sector.

5 Concluding remarks

We have introduced novel methodology for robust estimation of a conditional independence graph via γ -divergence. The method is designed for cell-wise contamination and is able to extract available information from multivariate data even when they are high-dimensional with corrupted values in many/most observations. Our method strongly outperformed competitors in our simulations. In particular, it showed very good behavior across different levels of contaminations.

A noteworthy result was found for the pairwise approach with Q_n ; recall (6). For asym-

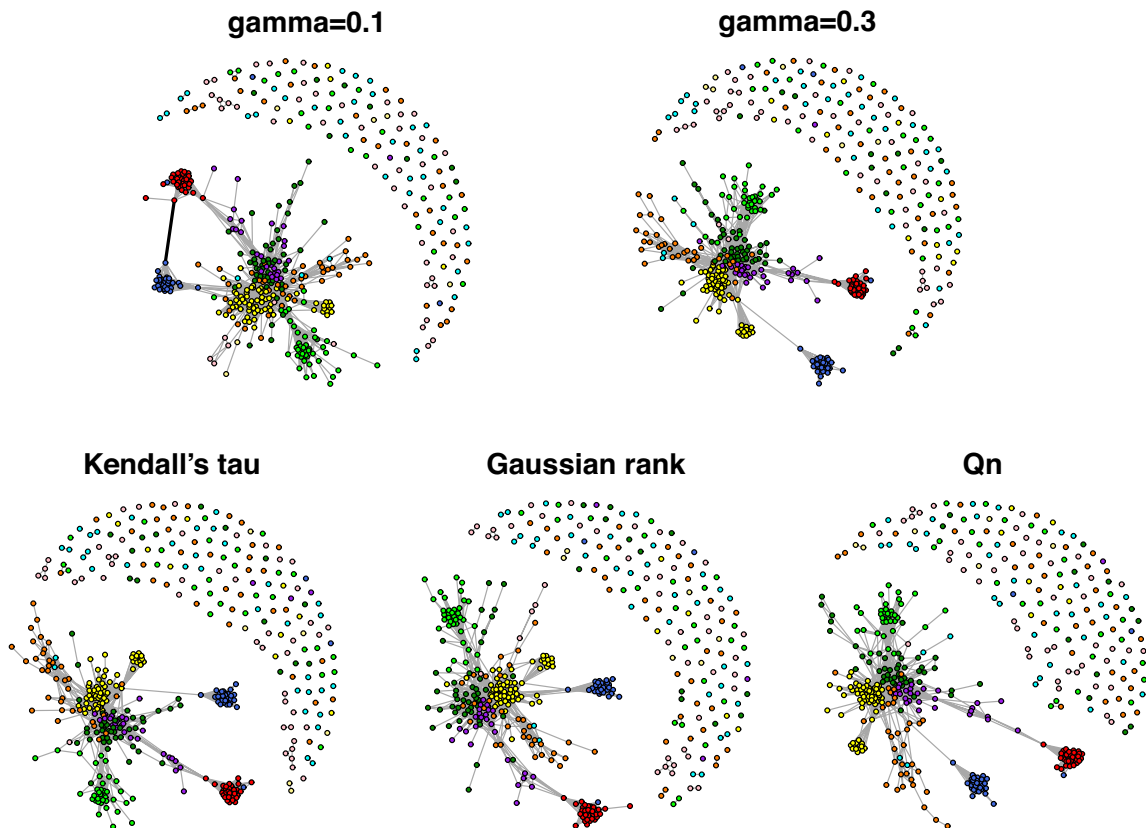


Figure 5: Graphs estimated with Glasso based on our estimator ($\gamma = 0.1, 0.3$), Kendall’s tau, Gaussian Rank and the pairwise approach with Q_n for the S&P 500 stock data set. Each graph has 2,500 edges. Each node represents a stock, and stocks from the same GICS sector have the same color. A stock in the “Utilities” (blue) sector links to a stock in the “Materials” (red) sector only for our method with $\gamma = 0.1$. This edge is drawn bold.

metric contamination it performed well even at high contamination levels, but it performed poorly for symmetric scenario. This imbalance can be explained as follows. For univariate samples X_1, \dots, X_n , the Q_n is based on the first quantile of $\{|X_i - X_j| : i < j\}$. If both X_i and X_j are contaminated as a $N(10, 1)$ draw, then the difference $X_i - X_j \sim N(0, 2)$ behaves as it does for clean observations. However, this is not the case for symmetric contamination with, say, $X_i \sim N(10, 1)$ and $X_j \sim N(-10, 1)$.

Our experiments in Section 4 show that our method can achieve good results with a fixed default value for divergence parameter γ . Of course, further improvements are possible by tuning this parameter. This, however, is challenging because an optimal choice of γ would depend on the typically unknown contamination density and level. If entirely clean subsamples were available, then γ could be tuned by comparing the sample covariance matrix

of the sub-samples and the robust covariance matrix obtained via γ -divergence of the other samples that may include contaminations.

For the simpler approach that uses rank correlations, [Loh & Tan \(2015\)](#) were able to give an analysis of the estimation error $\|\hat{\Sigma} - \Sigma\|_\infty$. Obtaining analogous results for the estimator via γ -divergence is an interesting open problem for future work. A key challenge is the non-convexity of the objective function, which makes the results of [Miao \(2010\)](#) and [Catoni \(2012\)](#) inapplicable. However, we believe that some convexity properties hold on a restricted parameter space and may offer a way to analyze the estimator.

Appendix A Projected gradient descent algorithm

We outline the projected gradient descent algorithm for computation of $\hat{\rho}_{jk}$ from (5). To avoid numerical singularity, we replace the restriction $|\rho_{jk}| < 1$ by $|\rho_{jk}| \leq R$ with $R \approx 1$. For simpler notation, let $d_\gamma(\rho_{jk}) = d_\gamma(f_n^{(j,k)}, h_{\rho_{jk}})$. The gradient of this function is

$$\nabla d_\gamma(\rho_{jk}) = \frac{\gamma}{(1 - \rho_{jk}^2)^2} \sum_{i=1}^n w_{ijk} \{ (1 + \rho_{jk}^2) Z_{ij} Z_{ik} - \rho_{jk} (Z_{ij}^2 + Z_{ik}^2) \} - \frac{1}{1 + \gamma} \frac{\rho_{jk}}{1 - \rho_{jk}^2},$$

where

$$w_{ijk} = \exp \left\{ -\frac{\gamma}{2(1 - \rho_{jk}^2)} (Z_{ij}^2 + Z_{ik}^2 - 2\rho_{jk} Z_{ij} Z_{ik}) \right\} / \sum_{i=1}^n \exp \left\{ -\frac{\gamma}{2(1 - \rho_{jk}^2)} (Z_{ij}^2 + Z_{ik}^2 - 2\rho_{jk} Z_{ij} Z_{ik}) \right\}.$$

The objective function $d_\gamma(\rho_{jk})$ is locally approximated around ρ'_{jk} by

$$\phi_\gamma(\rho_{jk}; \rho'_{jk}) = d_\gamma(\rho'_{jk}) + \nabla d_\gamma(\rho'_{jk})(\rho_{jk} - \rho'_{jk}) + \frac{s}{2}(\rho_{jk} - \rho'_{jk})^2,$$

where $s > 0$ is the step size parameter. We select sufficiently large s such that $d_\gamma(\rho_{jk}) \leq \phi_\gamma(\rho_{jk}; \rho'_{jk})$. The projected gradient descent minimizes $\phi_\gamma(\rho_{jk}; \rho'_{jk})$ over $|\rho_{jk}| \leq R$ instead of $d_\gamma(\rho_{jk})$. The minimizer is $\text{sgn}(\bar{\rho}'_{jk}) \min(|\bar{\rho}'_{jk}|, R)$ with $\bar{\rho}'_{jk} = \rho'_{jk} - s^{-1} \nabla d_\gamma(\rho'_{jk})$. Algorithm 1 summarizes the procedure.

References

Alqallaf, FA, Konis, KP, Martin, RD & Zamar, RH (2002), ‘Scalable robust covariance and correlation estimates for data mining’, In *Proceedings of the Eighth ACM SIGKDD International Conference on Knowledge Discovery and Data Mining*, pp.14–23. ACM, New York, NY, USA.

Algorithm 1: Projected gradient descent algorithm for $\hat{\rho}_{jk}$

Input: Standardized data $(Z_{1j}, Z_{1k}), \dots, (Z_{nj}, Z_{nk})$; divergence parameter $\gamma > 0$.
Initialize $t = 0$, $\rho_{jk}^0 = 0$, $s^0 = 0.01$ and set $R = 0.99$.

repeat

$t_{in} \leftarrow 0$
 $s^{t,t_{in}} \leftarrow s^t$

repeat

$\nu_{jk}^{t,t_{in}} \leftarrow \rho_{jk}^t - \nabla d_\gamma(\rho_{jk}^t) / s^{t,t_{in}}$
 $\rho_{jk}^{t,t_{in}+1} \leftarrow \text{sgn}(\nu_{jk}^{t,t_{in}}) \min(|\nu_{jk}^{t,t_{in}}|, R)$
 $s^{t,t_{in}+1} \leftarrow 2s^{t,t_{in}}$

$t_{in} \leftarrow t_{in} + 1$

until $d_\gamma(\rho_{jk}^t) \leq \phi_\gamma(\rho_{jk}^t; \rho_{jk}^{t,t_{in}})$;

$\rho_{jk}^{t+1} \leftarrow \rho_{jk}^{t,t_{in}}$
 $s^{t+1} \leftarrow s^{t,t_{in}} / 2$

$t \leftarrow t + 1$

until convergence;

Banerjee, O, El Ghaoui, L & D’Aspremont, A (2008), ‘Model selection through sparse maximum likelihood estimation for multivariate Gaussian or binary data’, *Journal of Machine Learning Research*, **9**, 485–516.

Bickel, PJ & Levina, E (2008), ‘Covariance regularization by thresholding’, *The Annals of Statistics*, **36**, 2577–2604.

Boudt, K, Cornelissen, J & Croux, C (2012), ‘The Gaussian rank correlation estimator: robustness properties’, *Statistics and Computing*, **22**, 471–483.

Cai, T, Liu, W & Luo, X (2011), ‘A constrained ℓ_1 minimization approach to sparse precision matrix estimation’, *Journal of the American Statistical Association*, **106**, 594–607.

Catoni, O (2012), ‘Challenging the empirical mean and empirical variance: a deviation study’, *Annales de l’Institut Henri Poincaré, Probabilités et Statistiques*, **48**, 1148–1185.

Drton, M & Maathuis, MH (2017), ‘Structure learning in graphical modeling’, *Annual Review of Statistics and Its Application*, **4**, 365–393.

Finegold, M & Drton, M (2011), ‘Robust graphical modeling of gene networks using classical and alternative t-distributions’, *The Annals of Applied Statistics*, **2A**, 1057–1080.

Finegold, M & Drton, M (2014), ‘Robust Bayesian graphical modeling using Dirichlet t-distributions’, *Bayesian Analysis*, **3**, 521–550.

- Friedman, JH, Hastie, T & Tibshirani, R (2008), ‘Sparse inverse covariance estimation with the graphical lasso’, *Biostatistics*, **9**, 432–441.
- Fujisawa, H & Eguchi, S (2008), ‘Robust parameter estimation with a small bias against heavy contamination’, *Journal of Multivariate Analysis*, **99**, 2053–2081.
- Gnanadesikan, R & Kettenring, JR (1972), ‘Robust estimates, residuals and outlier detection with multiresponse data’, *Biometrics*, **28**, 81–124.
- Hsieh, C-J, Sustik, MA, Dhillon, IS & Ravikumar, P (2011), ‘Sparse inverse covariance matrix estimation using quadratic approximation’, In *Advances in Neural Information Processing Systems*, pp. 2330–2338.
- Jeng, XJ & Daye, ZJ (2011), ‘Sparse covariance thresholding for high-dimensional variable selection’, *Statistica Sinica*, **21**, 625–657.
- Khare, K, Oh, S-Y & Rajaratnam, B (2015), ‘A convex pseudolikelihood framework for high dimensional partial correlation estimation with convergence guarantees’, *Journal of the Royal Statistical Society Series B*, **77**, 803–825.
- Lin, L, Drton, M & Shojaie, A (2016), ‘Estimation of high-dimensional graphical models using regularized score matching’, *Electronic Journal of Statistics*, **10**, 806–854.
- Liu, H, Han, F, Yuan, M & Lafferty, J (2012), ‘High-dimensional semiparametric Gaussian copula graphical models’, *The Annals of Statistics*, **40**, 2293–2326.
- Liu, X & Luo, X (2015), ‘Fast and adaptive sparse precision matrix estimation in high dimensions’, *Journal of Multivariate Analysis*, **135**, 153–162.
- Loh, P-L & Tan, XL (2015), ‘High-dimensional robust precision matrix estimation: Cellwise corruption under ε contamination’, *arXiv:1509.07229*.
- Maronna, RA & Zamar, RH (2002), ‘Robust estimates of location and dispersion for high-dimensional datasets’, *Technometrics*, **44**, 307–317.
- Maronna, RA, Martin, RD & Yohai, V (2006), *Robust Statistics: Theory and Methods*, Wiley, New York.
- Meinshausen, N & Bühlmann, P (2006), ‘High-dimensional graphs and variable selection with the lasso’, *The Annals of Statistics*, **34**, 1436–1462.

- Miao, O (2010), ‘Concentration inequality of maximum likelihood estimator’, *Applied Mathematics Letters*, **23**, 1305–1309.
- Öllerer, V & Croux, X (2015), ‘Robust high-dimensional precision matrix estimation’, In *Modern Nonparametric, Robust and Multivariate Methods*, pp. 325–350. Springer International Publishing.
- Peng, J, Wang, P, Zhou, N & Zhu, J (2009), ‘Partial correlation estimation by joint sparse regression models’, *Journal of the American Statistical Association*, **104**, 735–746.
- Ravikumar, P, Wainwright, MJ, Raskutti, G & Yu, B (2011), ‘High-dimensional covariance estimation by minimizing ℓ_1 -penalized log-determinant divergence’, *Electronic Journal of Statistics*, **5**, 935–980.
- Rousseeuw, PJ & Croux, C (1993), ‘Alternatives to the median absolute deviation’, *Journal of the American Statistical Association*, **88**, 1273–1283.
- Tarr, G, Müller, S & Weber, NC (2012), ‘A robust scale estimator based on pairwise means’, *Journal of Nonparametric Statistics*, **24**, 187–199.
- Tarr, G, Müller, S & Weber NC (2016), ‘Robust estimation of precision matrices under cellwise contamination’, *Computational Statistics and Data Analysis*, **93**, 404–420.
- Wille, A, Zimmermann, P, Vranová, E, Fürholz, A, Laule, O, Bleuler, S, Henning, L, Prelić, A, von Rohr, P, Thiele, L, Zitzler, E, Gruissem, W & Zitzler, E (2004), ‘Sparse graphical Gaussian modeling of the isoprenoid gene network in *Arabidopsis thaliana*’, *Genome biology*, **5**, R92.
- Yuan, M (2009), ‘Sparse inverse covariance matrix estimation via linear programming’, *Journal of Machine Learning Research*, **11**, 2261–2286.
- Yuan, M & Lin, Y (2007), ‘Model selection and estimation in the Gaussian graphical model’, *Biometrika*, **94**, 19–35.
- Zhang, T & Zou, H (2014), ‘Sparse precision matrix estimation via lasso penalized D-trace loss’, *Biometrika*, **101**, 103–120.
- Zhao, T, Liu, H, Roeder, K, Lafferty, J, & Wasserman, L (2012), ‘The huge package for high-dimensional undirected graph estimation in R’, *Journal of Machine Learning Research*, **13**, 1059–1062.

Zhao, T, Roeder, K, & Liu, H (2014), ‘Positive semidefinite rank-based correlation matrix estimation with application to semiparametric graph estimation’, *Journal of Computational and Graphical Statistics*, **23**, 895–922.

Supplementary article: Robust and sparse Gaussian graphical modeling under cell-wise contamination

Shota Katayama¹, Hironori Fujisawa^{2,3} and Mathias Drton⁴

¹Department of Industrial Engineering and Economics, Tokyo Institute of Technology, Japan

²The Institute of Statistical Mathematics, Japan

³Nagoya University Graduate School of Medicine, Japan

⁴Department of Statistics, University of Washington, USA

S1 Additional simulations

This supplementary article provides additional simulation results. The data generating process is the same as the article, except that we restrict the dimension to $p = 50$ for the CLIME simulation due to long computation time. The node-wise regression was carried out using the huge package of [Zhao et al. \(2012\)](#) and CLIME was computed with the `clime` package of [Cai et al. \(2011\)](#). We used the perturbation default set in the `clime` package. Negative definite robust covariance matrices were projected to positive semidefiniteness using the procedure from the main article.

S1.1 ROC curves

The ROC curves for the node-wise regression and CLIME are provided in [Figure S1](#) and [Figure S2](#). We observe behavior similarly to that discussed for the Glasso in the main article.

S1.2 Quantitative performances

Tables [S1](#) and [S2](#) summarize the performance of Glasso with the tuning parameter selected by the 2-fold cross validation when $\varepsilon = 0.05$ and $\varepsilon = 0.15$, respectively. The result for $\varepsilon = 0.25$ is reported in the article. For the low contamination level $\varepsilon = 0.05$, the five methods are comparable, but our method outperforms the competitors for higher contamination level. Tables [S3–S5](#) show the results of node-wise regression. The edge set was estimated by the "OR" rule, and the tuning parameter was selected by the Stability Approach for

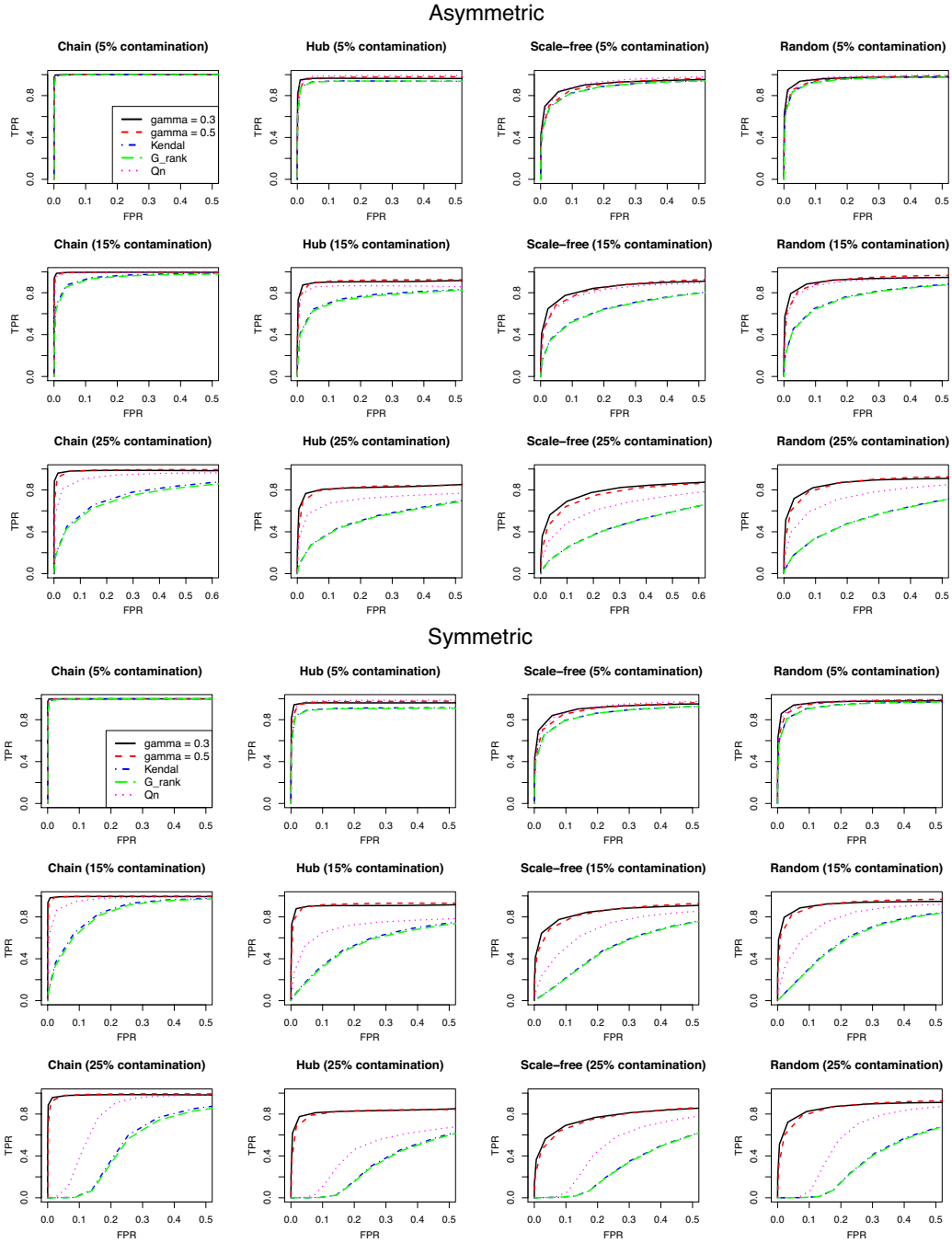


Figure S1: ROC curves for node-wise regression based on our estimators with $\gamma = 0.3$ and $\gamma = 0.5$, Kendall's tau, Gaussian rank and pairwise approach with Q_n , for asymmetric and symmetric contaminations at the different levels ($\varepsilon = 0.05, 0.15, 0.25$).

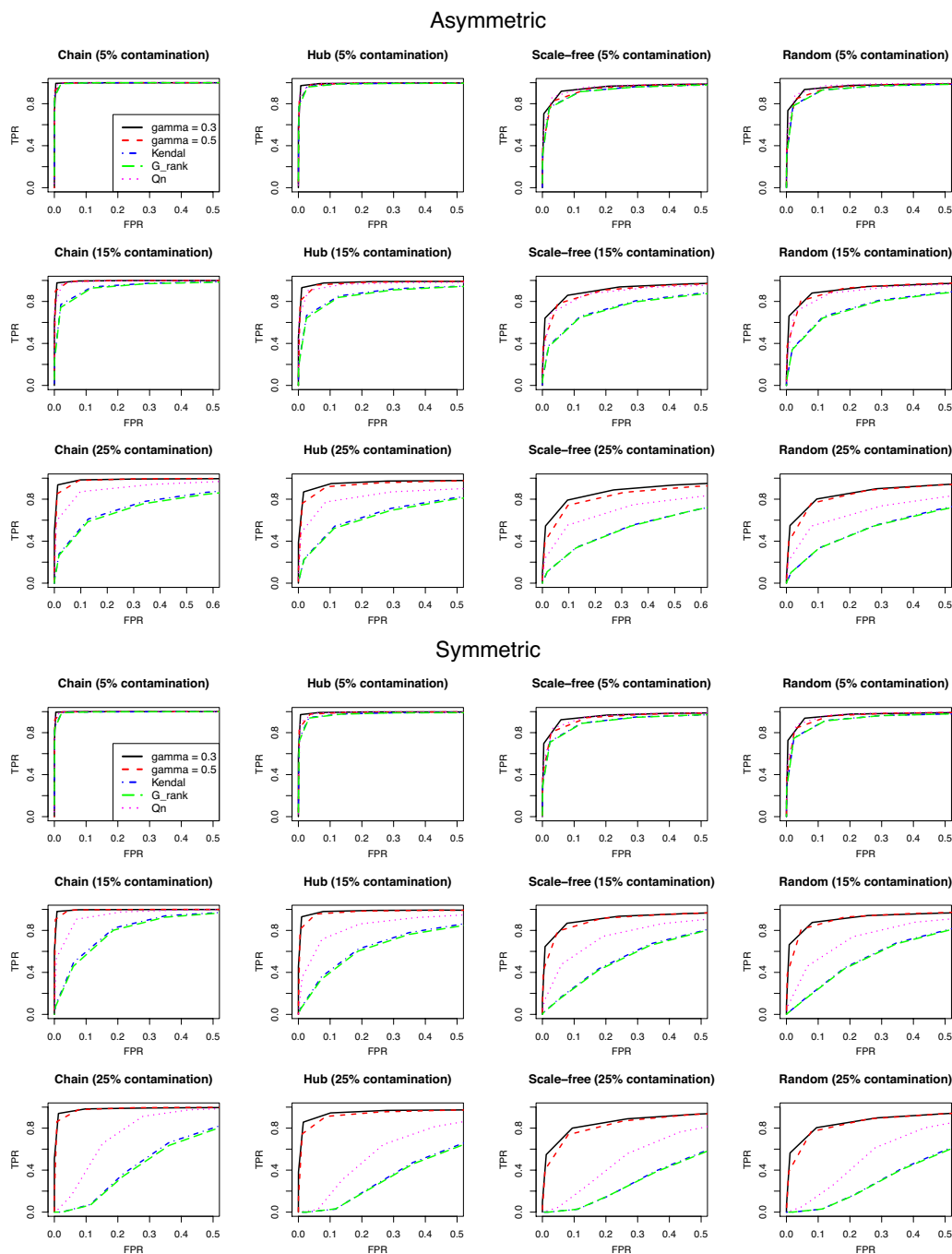


Figure S2: ROC curves for CLIME based on our estimators with $\gamma = 0.3$ and $\gamma = 0.5$, Kendall's tau, Gaussian rank and pairwise approach with Q_n , for asymmetric and symmetric contaminations at the different levels ($\varepsilon = 0.05, 0.15, 0.25$).

Regularization Selection (StARS, [Liu et al., 2010](#)) with 10 times sub-sampling to size $n/2$ and the cut point value 0.2. Tables [S6–S8](#) provide the results of CLIME with the tuning parameter selected by 2-fold cross validation. With both node-wise regression and CLIME, we see that the tuning parameter selection does not work well for Q_n when $\varepsilon = 0.25$, in contrast to the case of Glasso.

References

- Cai, T, Liu, W & Luo, X (2011), ‘A constrained ℓ_1 minimization approach to sparse precision matrix estimation’, *Journal of the American Statistical Association*, **106**, 594–607.
- Liu, H, Roeder, K & Wasserman, L (2010), ‘Stability approach to regularization selection for high dimensional graphical models’, *Advances in Neural Information Processing Systems*.
- Zhao, T, Liu, H, Roeder, K, Lafferty, J, & Wasserman, L (2012), ‘The huge package for high-dimensional undirected graph estimation in R’, *Journal of Machine Learning Research*, **13**, 1059–1062.

Table S1: Quantitative performances of Glasso based on the 5 methods when $\varepsilon = 0.05$ and the tuning parameter is selected by 2-fold cross validation. Each value shows the mean (standard deviation) on 100 simulated data set.

	Chain			Hub			Scale-free			Random			
	MSE	TPR	FPR	MSE	TPR	FPR	MSE	TPR	FPR	MSE	TPR	FPR	
Asym.	$\gamma = 0.3$	0.066	1.000	0.088	0.075	0.987	0.084	0.048	0.788	0.041	0.041	0.947	0.071
		(0.003)	(0.002)	(0.017)	(0.002)	(0.012)	(0.020)	(0.002)	(0.067)	(0.018)	(0.002)	(0.023)	(0.025)
	$\gamma = 0.5$	0.080	0.998	0.058	0.083	0.973	0.075	0.052	0.664	0.028	0.046	0.892	0.057
		(0.003)	(0.004)	(0.026)	(0.002)	(0.023)	(0.025)	(0.002)	(0.093)	(0.014)	(0.002)	(0.054)	(0.021)
	Kend	0.086	0.998	0.076	0.088	0.969	0.084	0.058	0.654	0.034	0.052	0.892	0.066
		(0.004)	(0.004)	(0.031)	(0.003)	(0.028)	(0.025)	(0.002)	(0.086)	(0.016)	(0.002)	(0.047)	(0.024)
Grank	0.088	0.997	0.067	0.089	0.963	0.078	0.059	0.638	0.032	0.052	0.877	0.059	
	(0.004)	(0.007)	(0.030)	(0.003)	(0.030)	(0.023)	(0.002)	(0.095)	(0.016)	(0.002)	(0.052)	(0.024)	
Q_n	0.097	0.999	0.059	0.095	0.982	0.076	0.062	0.689	0.027	0.056	0.925	0.057	
	(0.002)	(0.003)	(0.026)	(0.002)	(0.021)	(0.026)	(0.001)	(0.105)	(0.014)	(0.001)	(0.034)	(0.019)	
Sym.	$\gamma = 0.3$	0.066	1.000	0.087	0.076	0.984	0.083	0.048	0.786	0.039	0.041	0.948	0.070
		(0.003)	(0.002)	(0.016)	(0.002)	(0.014)	(0.022)	(0.002)	(0.062)	(0.017)	(0.002)	(0.021)	(0.023)
	$\gamma = 0.5$	0.080	0.999	0.059	0.083	0.969	0.074	0.052	0.661	0.026	0.046	0.888	0.055
		(0.003)	(0.004)	(0.025)	(0.002)	(0.029)	(0.025)	(0.002)	(0.095)	(0.013)	(0.002)	(0.063)	(0.025)
	Kend	0.088	0.998	0.071	0.090	0.949	0.088	0.059	0.647	0.036	0.052	0.867	0.066
		(0.004)	(0.005)	(0.030)	(0.003)	(0.033)	(0.026)	(0.002)	(0.097)	(0.016)	(0.002)	(0.056)	(0.026)
Grank	0.089	0.996	0.064	0.090	0.940	0.080	0.059	0.624	0.033	0.052	0.862	0.063	
	(0.004)	(0.006)	(0.027)	(0.003)	(0.042)	(0.028)	(0.002)	(0.106)	(0.016)	(0.002)	(0.056)	(0.024)	
Q_n	0.097	0.999	0.060	0.095	0.979	0.086	0.062	0.699	0.031	0.056	0.905	0.055	
	(0.002)	(0.003)	(0.026)	(0.002)	(0.022)	(0.025)	(0.001)	(0.091)	(0.014)	(0.001)	(0.051)	(0.022)	

Table S2: Quantitative performance of Glasso based on the 5 methods when $\varepsilon = 0.15$ and the tuning parameter is selected by 2-fold cross validation. Each value shows the mean (standard deviation) on 100 simulated data sets.

	Chain			Hub			Scale-free			Random			
	MSE	TPR	FPR	MSE	TPR	FPR	MSE	TPR	FPR	MSE	TPR	FPR	
Asym.	$\gamma = 0.3$	0.068	0.999	0.099	0.079	0.957	0.087	0.051	0.681	0.040	0.043	0.894	0.073
		(0.003)	(0.004)	(0.019)	(0.002)	(0.022)	(0.022)	(0.002)	(0.075)	(0.018)	(0.002)	(0.031)	(0.021)
	$\gamma = 0.5$	0.083	0.993	0.056	0.087	0.917	0.060	0.054	0.520	0.022	0.049	0.783	0.041
		(0.003)	(0.010)	(0.022)	(0.002)	(0.048)	(0.024)	(0.002)	(0.113)	(0.014)	(0.002)	(0.072)	(0.020)
	Kend	0.120	0.832	0.037	0.113	0.564	0.034	0.078	0.226	0.016	0.071	0.387	0.023
		(0.002)	(0.076)	(0.015)	(0.002)	(0.144)	(0.021)	(0.002)	(0.092)	(0.011)	(0.001)	(0.107)	(0.015)
Grank	0.120	0.805	0.035	0.113	0.555	0.033	0.078	0.203	0.013	0.072	0.361	0.020	
	(0.002)	(0.084)	(0.015)	(0.002)	(0.136)	(0.019)	(0.002)	(0.094)	(0.010)	(0.001)	(0.110)	(0.014)	
Q_n	0.119	0.996	0.094	0.114	0.929	0.082	0.083	0.613	0.041	0.073	0.842	0.074	
	(0.002)	(0.006)	(0.030)	(0.002)	(0.034)	(0.026)	(0.001)	(0.087)	(0.018)	(0.001)	(0.057)	(0.025)	
Sym.	$\gamma = 0.3$	0.069	0.998	0.101	0.079	0.961	0.093	0.050	0.704	0.044	0.043	0.899	0.076
		(0.002)	(0.004)	(0.018)	(0.002)	(0.020)	(0.021)	(0.002)	(0.073)	(0.020)	(0.002)	(0.032)	(0.021)
	$\gamma = 0.5$	0.083	0.992	0.053	0.087	0.910	0.059	0.054	0.546	0.024	0.049	0.783	0.043
		(0.002)	(0.010)	(0.018)	(0.002)	(0.053)	(0.025)	(0.002)	(0.114)	(0.015)	(0.002)	(0.076)	(0.022)
	Kend	0.117	0.698	0.141	0.110	0.416	0.155	0.074	0.177	0.113	0.068	0.283	0.124
		(0.002)	(0.083)	(0.034)	(0.001)	(0.080)	(0.026)	(0.001)	(0.069)	(0.035)	(0.001)	(0.076)	(0.031)
Grank	0.117	0.648	0.130	0.110	0.385	0.148	0.074	0.166	0.111	0.068	0.269	0.123	
	(0.002)	(0.088)	(0.032)	(0.001)	(0.085)	(0.026)	(0.001)	(0.065)	(0.036)	(0.001)	(0.068)	(0.030)	
Q_n	0.120	0.988	0.199	0.116	0.791	0.173	0.083	0.501	0.116	0.074	0.748	0.170	
	(0.002)	(0.012)	(0.033)	(0.001)	(0.051)	(0.025)	(0.001)	(0.097)	(0.035)	(0.001)	(0.057)	(0.031)	

Table S3: Quantitative performance of node-wise regression based on the 5 methods when $\varepsilon = 0.05$ and the tuning parameter is selected by StARS. Each value shows the mean (standard deviation) on 100 simulated data sets.

		Chain		Hub		Scale-free		Random	
		TPR	FPR	TPR	FPR	TPR	FPR	TPR	FPR
Asym.	$\gamma = 0.3$	1.000	0.059	0.958	0.053	0.805	0.042	0.936	0.053
		(0.002)	(0.018)	(0.022)	(0.015)	(0.056)	(0.019)	(0.027)	(0.016)
	$\gamma = 0.5$	0.998	0.028	0.949	0.038	0.712	0.032	0.848	0.028
		(0.005)	(0.012)	(0.031)	(0.016)	(0.076)	(0.014)	(0.047)	(0.014)
	Kend	0.996	0.038	0.921	0.046	0.684	0.032	0.868	0.042
		(0.006)	(0.019)	(0.029)	(0.017)	(0.080)	(0.017)	(0.046)	(0.016)
	Grank	0.996	0.037	0.920	0.045	0.658	0.028	0.862	0.041
		(0.006)	(0.020)	(0.031)	(0.017)	(0.106)	(0.016)	(0.048)	(0.016)
	Q_n	0.999	0.036	0.975	0.036	0.747	0.029	0.894	0.028
		(0.002)	(0.012)	(0.017)	(0.015)	(0.082)	(0.013)	(0.039)	(0.011)
Sym.	$\gamma = 0.3$	1.000	0.056	0.962	0.051	0.797	0.041	0.934	0.049
		(0.002)	(0.018)	(0.018)	(0.015)	(0.063)	(0.019)	(0.025)	(0.016)
	$\gamma = 0.5$	0.998	0.025	0.958	0.041	0.685	0.026	0.862	0.030
		(0.006)	(0.011)	(0.025)	(0.017)	(0.074)	(0.012)	(0.050)	(0.014)
	Kend	0.995	0.042	0.895	0.050	0.649	0.034	0.827	0.041
		(0.008)	(0.021)	(0.039)	(0.016)	(0.072)	(0.015)	(0.053)	(0.019)
	Grank	0.994	0.039	0.889	0.047	0.636	0.031	0.814	0.038
		(0.009)	(0.021)	(0.042)	(0.015)	(0.078)	(0.014)	(0.059)	(0.018)
	Q_n	0.999	0.035	0.973	0.039	0.714	0.028	0.882	0.030
		(0.003)	(0.011)	(0.017)	(0.015)	(0.084)	(0.014)	(0.052)	(0.013)

Table S4: Quantitative performance of node-wise regression based on the 5 methods when $\varepsilon = 0.15$ and the tuning parameter is selected by StARS. Each value shows the mean (standard deviation) on 100 simulated data sets.

		Chain		Hub		Scale-free		Random	
		TPR	FPR	TPR	FPR	TPR	FPR	TPR	FPR
Asym.	$\gamma = 0.3$	0.993	0.065	0.887	0.064	0.722	0.048	0.859	0.055
		(0.009)	(0.024)	(0.029)	(0.017)	(0.067)	(0.019)	(0.044)	(0.021)
	$\gamma = 0.5$	0.992	0.035	0.872	0.039	0.604	0.031	0.749	0.028
		(0.008)	(0.013)	(0.038)	(0.016)	(0.080)	(0.014)	(0.058)	(0.012)
	Kend	0.849	0.035	0.610	0.039	0.355	0.033	0.462	0.034
		(0.057)	(0.018)	(0.085)	(0.014)	(0.092)	(0.016)	(0.079)	(0.015)
	Grank	0.818	0.031	0.597	0.039	0.341	0.031	0.441	0.031
		(0.066)	(0.017)	(0.085)	(0.013)	(0.094)	(0.015)	(0.085)	(0.014)
	Q_n	0.989	0.046	0.855	0.049	0.636	0.042	0.765	0.038
		(0.012)	(0.018)	(0.040)	(0.019)	(0.067)	(0.017)	(0.058)	(0.018)
Sym.	$\gamma = 0.3$	0.995	0.058	0.895	0.064	0.725	0.052	0.869	0.056
		(0.007)	(0.024)	(0.026)	(0.017)	(0.073)	(0.021)	(0.034)	(0.019)
	$\gamma = 0.5$	0.990	0.034	0.881	0.038	0.584	0.027	0.778	0.032
		(0.009)	(0.014)	(0.035)	(0.016)	(0.078)	(0.012)	(0.058)	(0.014)
	Kend	0.626	0.079	0.285	0.082	0.151	0.068	0.203	0.067
		(0.077)	(0.018)	(0.071)	(0.017)	(0.064)	(0.023)	(0.075)	(0.023)
	Grank	0.583	0.075	0.278	0.083	0.143	0.065	0.189	0.064
		(0.084)	(0.019)	(0.072)	(0.017)	(0.063)	(0.023)	(0.077)	(0.023)
	Q_n	0.950	0.091	0.623	0.083	0.425	0.067	0.561	0.073
		(0.029)	(0.023)	(0.060)	(0.021)	(0.080)	(0.018)	(0.075)	(0.020)

Table S5: Quantitative performance of node-wise regression based on the 5 methods when $\varepsilon = 0.25$ and the tuning parameter is selected by StARS. Each value shows the mean (standard deviation) on 100 simulated data sets.

		Chain		Hub		Scale-free		Random	
		TPR	FPR	TPR	FPR	TPR	FPR	TPR	FPR
Asym.	$\gamma = 0.3$	0.978 (0.013)	0.059 (0.024)	0.799 (0.042)	0.071 (0.020)	0.614 (0.065)	0.057 (0.019)	0.776 (0.060)	0.062 (0.021)
	$\gamma = 0.5$	0.972 (0.019)	0.046 (0.016)	0.757 (0.046)	0.044 (0.019)	0.530 (0.090)	0.041 (0.019)	0.680 (0.075)	0.042 (0.017)
	Kend	0.391 (0.087)	0.031 (0.014)	0.241 (0.071)	0.034 (0.014)	0.136 (0.051)	0.031 (0.014)	0.188 (0.066)	0.036 (0.016)
	Grank	0.367 (0.088)	0.030 (0.013)	0.228 (0.071)	0.031 (0.013)	0.132 (0.051)	0.029 (0.013)	0.174 (0.065)	0.032 (0.015)
	Q_n	0.881 (0.043)	0.062 (0.022)	0.642 (0.063)	0.063 (0.023)	0.429 (0.069)	0.058 (0.019)	0.547 (0.069)	0.059 (0.020)
Sym.	$\gamma = 0.3$	0.977 (0.016)	0.063 (0.027)	0.806 (0.038)	0.075 (0.019)	0.622 (0.062)	0.059 (0.021)	0.782 (0.047)	0.066 (0.020)
	$\gamma = 0.5$	0.975 (0.018)	0.047 (0.016)	0.765 (0.053)	0.047 (0.019)	0.526 (0.084)	0.041 (0.016)	0.678 (0.067)	0.040 (0.017)
	Kend	0.068 (0.050)	0.134 (0.019)	0.031 (0.023)	0.144 (0.017)	0.023 (0.019)	0.137 (0.020)	0.016 (0.016)	0.132 (0.020)
	Grank	0.057 (0.044)	0.132 (0.020)	0.026 (0.023)	0.140 (0.019)	0.024 (0.020)	0.137 (0.020)	0.014 (0.014)	0.130 (0.019)
	Q_n	0.600 (0.116)	0.137 (0.018)	0.221 (0.065)	0.135 (0.013)	0.137 (0.066)	0.132 (0.015)	0.183 (0.094)	0.132 (0.019)

Table S6: Quantitative performance of CLIME based on the 5 methods when $\varepsilon = 0.05$ and the tuning parameter is selected by 2-fold cross validation. Each value shows the mean (standard deviation) on 100 simulated data sets.

		Chain			Hub			Scale-free			Random		
		MSE	TPR	FPR	MSE	TPR	FPR	MSE	TPR	FPR	MSE	TPR	FPR
Asym.	$\gamma = 0.3$	0.067 (0.007)	0.999 (0.005)	0.098 (0.046)	0.072 (0.006)	0.994 (0.011)	0.100 (0.039)	0.058 (0.006)	0.910 (0.053)	0.071 (0.039)	0.048 (0.005)	0.948 (0.027)	0.099 (0.045)
	$\gamma = 0.5$	0.105 (0.006)	0.995 (0.011)	0.034 (0.023)	0.115 (0.005)	0.976 (0.022)	0.045 (0.025)	0.079 (0.005)	0.789 (0.098)	0.032 (0.020)	0.064 (0.005)	0.840 (0.086)	0.037 (0.024)
	Kend	0.105 (0.007)	0.997 (0.008)	0.067 (0.033)	0.112 (0.008)	0.974 (0.026)	0.073 (0.036)	0.084 (0.007)	0.797 (0.109)	0.047 (0.033)	0.068 (0.005)	0.872 (0.075)	0.062 (0.036)
	Grank	0.110 (0.008)	0.994 (0.012)	0.052 (0.030)	0.114 (0.008)	0.971 (0.031)	0.068 (0.033)	0.086 (0.008)	0.748 (0.143)	0.037 (0.030)	0.070 (0.005)	0.855 (0.070)	0.051 (0.031)
	Q_n	0.129 (0.003)	0.999 (0.005)	0.057 (0.029)	0.135 (0.004)	0.992 (0.013)	0.086 (0.036)	0.095 (0.003)	0.865 (0.070)	0.044 (0.027)	0.077 (0.003)	0.922 (0.053)	0.058 (0.031)
Sym.	$\gamma = 0.3$	0.067 (0.007)	1.000 (0.005)	0.098 (0.046)	0.071 (0.006)	0.995 (0.011)	0.102 (0.039)	0.057 (0.006)	0.923 (0.053)	0.082 (0.039)	0.047 (0.005)	0.950 (0.027)	0.102 (0.045)
	$\gamma = 0.5$	0.104 (0.006)	0.996 (0.011)	0.038 (0.023)	0.114 (0.005)	0.980 (0.022)	0.050 (0.025)	0.080 (0.005)	0.773 (0.098)	0.030 (0.020)	0.063 (0.005)	0.866 (0.086)	0.044 (0.024)
	Kend	0.107 (0.007)	0.995 (0.008)	0.074 (0.033)	0.114 (0.008)	0.964 (0.026)	0.086 (0.036)	0.085 (0.007)	0.756 (0.109)	0.045 (0.033)	0.070 (0.005)	0.831 (0.075)	0.059 (0.036)
	Grank	0.111 (0.008)	0.992 (0.012)	0.055 (0.030)	0.118 (0.008)	0.950 (0.031)	0.074 (0.033)	0.086 (0.008)	0.747 (0.143)	0.043 (0.030)	0.071 (0.005)	0.814 (0.070)	0.052 (0.031)
	Q_n	0.130 (0.003)	0.999 (0.005)	0.057 (0.029)	0.137 (0.004)	0.989 (0.013)	0.078 (0.036)	0.096 (0.003)	0.842 (0.070)	0.046 (0.027)	0.078 (0.003)	0.915 (0.053)	0.067 (0.031)

Table S7: Quantitative performance of CLIME based on the 5 methods when $\varepsilon = 0.15$ and the tuning parameter is selected by 2-fold cross validation. Each value shows the mean (standard deviation) on 100 simulated data sets.

	Chain			Hub			Scale-free			Random			
	MSE	TPR	FPR	MSE	TPR	FPR	MSE	TPR	FPR	MSE	TPR	FPR	
Asym.	$\gamma = 0.3$	0.082	0.994	0.080	0.090	0.974	0.087	0.065	0.849	0.072	0.055	0.871	0.086
		(0.008)	(0.011)	(0.032)	(0.009)	(0.027)	(0.035)	(0.006)	(0.069)	(0.035)	(0.004)	(0.045)	(0.034)
	$\gamma = 0.5$	0.104	0.991	0.054	0.113	0.946	0.065	0.080	0.731	0.043	0.065	0.780	0.047
		(0.007)	(0.014)	(0.029)	(0.006)	(0.032)	(0.032)	(0.005)	(0.113)	(0.028)	(0.004)	(0.084)	(0.027)
	Kend	0.164	0.770	0.030	0.166	0.623	0.033	0.122	0.302	0.019	0.100	0.339	0.022
		(0.005)	(0.132)	(0.022)	(0.005)	(0.165)	(0.029)	(0.004)	(0.149)	(0.021)	(0.003)	(0.148)	(0.018)
Grank	0.166	0.687	0.022	0.168	0.538	0.023	0.123	0.260	0.014	0.101	0.303	0.017	
	(0.005)	(0.179)	(0.020)	(0.005)	(0.180)	(0.023)	(0.004)	(0.153)	(0.016)	(0.003)	(0.132)	(0.014)	
Q_n	0.162	0.989	0.075	0.162	0.929	0.076	0.122	0.756	0.059	0.100	0.817	0.074	
	(0.006)	(0.015)	(0.034)	(0.006)	(0.042)	(0.039)	(0.004)	(0.096)	(0.032)	(0.003)	(0.069)	(0.034)	
Sym.	$\gamma = 0.3$	0.081	0.996	0.094	0.089	0.975	0.087	0.064	0.840	0.069	0.055	0.875	0.083
		(0.008)	(0.011)	(0.032)	(0.009)	(0.027)	(0.035)	(0.006)	(0.069)	(0.035)	(0.004)	(0.045)	(0.034)
	$\gamma = 0.5$	0.105	0.991	0.053	0.114	0.950	0.067	0.080	0.715	0.038	0.065	0.777	0.049
		(0.007)	(0.014)	(0.029)	(0.006)	(0.032)	(0.032)	(0.005)	(0.113)	(0.028)	(0.004)	(0.084)	(0.027)
	Kend	0.158	0.669	0.124	0.160	0.502	0.136	0.115	0.241	0.096	0.095	0.268	0.109
		(0.005)	(0.132)	(0.022)	(0.005)	(0.165)	(0.029)	(0.004)	(0.149)	(0.021)	(0.003)	(0.148)	(0.018)
Grank	0.160	0.605	0.109	0.162	0.442	0.118	0.117	0.197	0.081	0.097	0.204	0.081	
	(0.005)	(0.179)	(0.020)	(0.005)	(0.180)	(0.023)	(0.004)	(0.153)	(0.016)	(0.003)	(0.132)	(0.014)	
Q_n	0.168	0.949	0.140	0.171	0.822	0.151	0.128	0.596	0.115	0.105	0.627	0.137	
	(0.006)	(0.015)	(0.034)	(0.006)	(0.042)	(0.039)	(0.004)	(0.096)	(0.032)	(0.003)	(0.069)	(0.034)	

Table S8: Quantitative performance of CLIME based on the 5 methods when $\varepsilon = 0.25$ and the tuning parameter is selected by 2-fold cross validation. Each value shows the mean (standard deviation) on 100 simulated data sets.

	Chain			Hub			Scale-free			Random			
	MSE	TPR	FPR	MSE	TPR	FPR	MSE	TPR	FPR	MSE	TPR	FPR	
Asym.	$\gamma = 0.3$	0.099	0.955	0.079	0.104	0.931	0.086	0.079	0.732	0.079	0.072	0.683	0.129
		(0.014)	(0.149)	(0.066)	(0.013)	(0.101)	(0.076)	(0.012)	(0.120)	(0.115)	(0.012)	(0.251)	(0.195)
	$\gamma = 0.5$	0.111	0.951	0.048	0.119	0.885	0.059	0.084	0.599	0.037	0.070	0.627	0.041
		(0.008)	(0.043)	(0.029)	(0.008)	(0.069)	(0.030)	(0.005)	(0.105)	(0.023)	(0.005)	(0.123)	(0.026)
	Kend	0.197	0.154	0.009	0.195	0.107	0.009	0.148	0.049	0.006	0.122	0.048	0.006
		(0.003)	(0.132)	(0.014)	(0.003)	(0.102)	(0.015)	(0.002)	(0.059)	(0.009)	(0.002)	(0.064)	(0.009)
Grank	0.198	0.101	0.004	0.196	0.094	0.007	0.149	0.036	0.004	0.123	0.032	0.003	
	(0.002)	(0.103)	(0.007)	(0.003)	(0.103)	(0.013)	(0.002)	(0.052)	(0.008)	(0.002)	(0.043)	(0.006)	
Q_n	0.192	0.878	0.100	0.191	0.768	0.097	0.149	0.519	0.074	0.121	0.544	0.089	
	(0.004)	(0.061)	(0.048)	(0.004)	(0.075)	(0.048)	(0.003)	(0.103)	(0.037)	(0.003)	(0.100)	(0.045)	
Sym.	$\gamma = 0.3$	0.096	0.979	0.075	0.103	0.934	0.077	0.077	0.724	0.059	0.066	0.734	0.057
		(0.014)	(0.149)	(0.066)	(0.013)	(0.101)	(0.076)	(0.012)	(0.120)	(0.115)	(0.012)	(0.251)	(0.195)
	$\gamma = 0.5$	0.112	0.958	0.048	0.119	0.886	0.054	0.084	0.581	0.034	0.070	0.615	0.040
		(0.008)	(0.043)	(0.029)	(0.008)	(0.069)	(0.030)	(0.005)	(0.105)	(0.023)	(0.005)	(0.123)	(0.026)
	Kend	0.171	0.592	0.319	0.171	0.436	0.337	0.124	0.308	0.301	0.102	0.336	0.316
		(0.003)	(0.132)	(0.014)	(0.003)	(0.102)	(0.015)	(0.002)	(0.059)	(0.009)	(0.002)	(0.064)	(0.009)
Grank	0.171	0.562	0.312	0.171	0.397	0.324	0.124	0.303	0.302	0.103	0.301	0.302	
	(0.002)	(0.103)	(0.007)	(0.003)	(0.103)	(0.013)	(0.002)	(0.052)	(0.008)	(0.002)	(0.043)	(0.006)	
Q_n	0.203	0.697	0.172	0.203	0.313	0.144	0.156	0.301	0.157	0.131	0.138	0.096	
	(0.004)	(0.061)	(0.048)	(0.004)	(0.075)	(0.048)	(0.003)	(0.103)	(0.037)	(0.003)	(0.100)	(0.045)	